

1 **Mitigating drought mortality by incorporating topography into variable forest thinning
2 strategies**

3 Anooja Thomas¹, Thomas Kolb², Joel Biederman³, Martin D. Venturas⁴, Qin Ma^{5,6,7}, Di Yang⁸,
4 Sabina Dore², Xiaonan Tai¹

5 ¹Department of Biological Sciences, New Jersey Institute of Technology, Newark, NJ, USA

6 ²School of Forestry, Northern Arizona University, Flagstaff, AZ, USA

7 ³Southwest Watershed Research Center, USDA Agricultural Research Service, Tucson, AZ,
8 USA

9 ⁴Departamento de Sistemas y Recursos Naturales, Universidad Politécnica de Madrid, Madrid,
10 Spain

11 ⁵School of Geography, Nanjing Normal University, Nanjing, China

12 ⁶Key Laboratory of Virtual Geographic Environment (Nanjing Normal University), Ministry of
13 Education, Nanjing, 210023, China

14 ⁷Jiangsu Center for Collaborative Innovation in Geographical Information Resource
15 Development and Application, Nanjing, 210023, China

16 ⁸Wyoming Geographic Information Science Center, University of Wyoming, Laramie, WY,
17 USA

18 Author for correspondence: Xiaonan Tai (xiaonan.tai@njit.edu)

19 **Abstract**

20
21 Drought-induced productivity reductions and tree mortality have been increasing in recent
22 decades in forests around the globe. Developing adaptation strategies hinges on an adequate
23 understanding of the mechanisms governing the drought vulnerability of forest stands. Prescribed
24 reduction in stand density has been used as a management tool to reduce water stress and
25 wildfire risk, but the processes that modulate fine-scale variations in plant water supply and
26 water demand are largely missing in ecosystem models. We used an ecohydrological model that
27 couples plant hydraulics with groundwater hydrology to examine how within-stand variations in
28 tree spatial arrangements and topography might mitigate forest vulnerability to drought at
29 individual-tree and stand scales. Our results demonstrated thinning generally ameliorated plant
30 hydraulic stress and improved carbon and water fluxes of the remaining trees, although the
31 effectiveness varied by climate and topography. Variable thinning that adjusted thinning

32 intensity based on topography-mediated water availability achieved higher stand productivity
33 and lower mortality risk, compared to evenly-spaced thinning at comparable intensities. The
34 results from numerical experiments provided mechanistic evidence that topography mediates the
35 effectiveness of thinning and highlighted the need for an explicit consideration of within-stand
36 heterogeneity in trees and abiotic environments when designing forest thinning to mitigate
37 drought impacts.
38

39 **Key words**

40 Drought mitigation; Thinning treatments; Tree neighborhood; Topography; Ecohydrological
41 modeling; Mortality risk

42 **Introduction**

43 Forests globally deliver critical ecosystem services such as provision of timber, fuel, and water,
44 regulation of climate and hydrology, and support of biodiversity [1, 2]. Anthropogenic climate
45 changes are threatening forests globally [3] due to increasing wildfires [4], insect outbreaks [5]
46 and widespread tree die-offs from drought and warming climate [6-8]. Future climate projections
47 suggest increasing drought frequency and intensity in most parts of the world [9, 10], with
48 serious consequences on the sustainability of forest functions and services [11]. Therefore, it is
49 crucial to develop effective mitigation strategies that minimize forest vulnerability to
50 unprecedented moisture deficits [12-14].

51 Considerable research has investigated the physiological mechanisms underlying climate-
52 induced mortality at the individual tree level [15, 16]. In particular, hydraulic damage refers to
53 the accumulation of emboli in the xylem that disrupts water transport and leads to cell death by
54 dehydration [17]. Models that explicitly simulate plant hydraulic impairments (e.g., percentage
55 loss of hydraulic conductance) were able to explain the mortality of different species with
56 contrasting vulnerability to cavitation [18], rooting depth [19], and drought treatments [20].
57 However, our understandings of the processes mediating mortality risks at stand or landscape
58 scales remain limited [21, 22]. The effects of climate stressors such as drought are filtered
59 through fine-grained attributes such as topography, soil heterogeneity, and tree neighborhoods
60 that mediate the realized microenvironment that individual trees experience, which may link to
61 tree-to-tree variations in mortality risks, and physiological functions such as water and carbon
62 fluxes [14, 23-25].

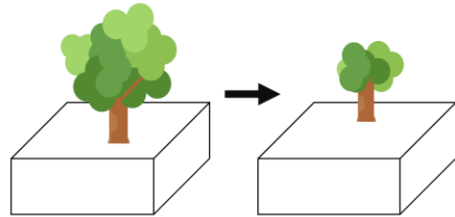
63 Stand density reduction through prescribed forest thinning has been employed to mitigate
64 drought impacts, promote tree- and stand-level growth and forest resilience to disturbances [26-
65 31]. Studies have shown high levels of competition within a forest stand can compound the
66 effects of drought and increase the probability of mortality, especially when water is a limiting
67 resource [32-34]. There is broad consensus that thinning potentially reduces total stand water
68 use, increases the water availability for remaining trees, and reduces inter-tree competition for
69 resources [12, 35-37]. Yet, few process-based vegetation models explicitly account for
70 competition for water among neighboring trees. Thinning treatments in most vegetation models
71 have been simplified as a decrease in biomass or leaf area at the stand scale (Figure 1a) [38-40]
72 and do not explicitly distinguish the changes in water availability experienced by an individual
73 tree as influenced by interactions with surrounding trees (Figure 1b).

74 Topography interacts with broader-scale climate to create spatially heterogeneous fine-scale
75 environments [41] that mediate individual tree responses to drought. Hydrologic processes such
76 as lateral flows of groundwater create drier hills and wetter valleys [42]. The systematic
77 variations in water availability driven by topography have emerged to be an important
78 mechanism mediating the spatial patterns of vegetation biomass [43], leaf area index [44],
79 sensitivity to drought [45], and drought-induced tree mortality [46, 47]. Despite its importance
80 and the preponderance of forests in mountain ranges [48], most vegetation models only represent
81 vertical flow through the soil matrix, whereas the impacts of terrain-mediated groundwater flow
82 on forest functions are ignored [49], limiting our ability to develop realistic estimations of plant
83 water supply. Further, topography is rarely accounted for or incorporated into thinning strategies.
84 For example, variable thinning that adjusts the inter-tree spacing based on elevation gradients has
85 been proposed [50], but it is not clear whether variable thinning would effectively mitigate
86 drought impacts on forests (Figure 1cd).

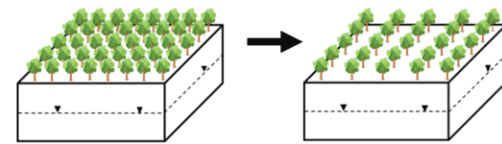
87
88 Effective forest management hinges on tools that can quantify tree mortality risks and
89 physiological functions in response to stand structure changes [6, 31]. Little research has been
90 directed specifically toward evaluating potential forest management options under different
91 climate scenarios, likely due to the lack of models that are able to capture relevant mechanisms.
92 Most vegetation models simulate the functioning of an “average stand” in each model grid cell
93 and do not account for the effects of fine-scale, within-grid cell variations in tree arrangements
94 and the influence of topography on plant water supply and mortality risk was ignored. This
95 leaves key knowledge gaps regarding the interactive effects of tree arrangements and topography
96 on forest vulnerability to various climatic conditions and hampers efforts to develop climate-
97 adapted management strategies on forested hillslopes.

98 This study employed a state-of-the-art, integrated plant hydraulics-hydrology model to
99 investigate how within-stand variations in tree arrangements and terrain could mediate responses
100 to climate variability from individual-tree scales up to forest stands. Parallel Flow-Terrestrial
101 Regional Ecosystem Exchange Simulator (ParFlow-TREES) simulates the transient, three-
102 dimensional water flux in the subsurface and along the soil-plant-atmospheric continuum at
103 individual-tree level [51, 52]. In addition to carbon and water fluxes, ParFlow-TREES estimates
104 the percentage of plant hydraulic damage, which has been shown to be a proxy of drought-
105 induced mortality risk for various vascular species by integrating the effects of water availability,
106 atmospheric demand, and plant hydraulic traits [53, 54]. We focused on a ponderosa pine (*Pinus*
107 *ponderosa*)-dominated ecosystem in northern Arizona with five-year eddy covariance
108 measurements of ecosystem water and carbon fluxes along with detailed meteorological
109 conditions, but the implications of our results are broadly applicable for other montane forest
110 management. Using ParFlow-TREES as a virtual laboratory, the goal of this study is to
111 experiment with different scenarios of tree arrangements, topography, and climate to disentangle
112 the multiple, interacting controls on forest water use, productivity, and vulnerability to drought.
113 Specifically, we asked: (1) How would lumped and explicit representation of thinning influence
114 tree functions and mortality risk? (2) How does topography interact with thinning to influence
115 forest responses to climate? And (3) Does variable thinning based on terrain result in enhanced
116 resistance to drought?

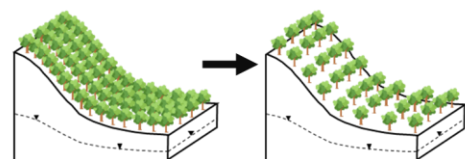
118 (a) Lumped stand thinning



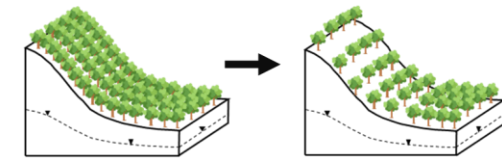
(b) Even thinning on flat terrain



(c) Even thinning on hillslope



(d) Variable thinning on hillslope



118

119 Figure 1. Conceptual diagram illustrating different representations of forest thinning with
 120 increasing complexity. (a) represents the commonly adopted modeling approach, where stand-
 121 level leaf area or basal area is decreased in a lumped mode, without explicit considerations of
 122 removing individual trees. (b) represents spatially explicit thinning that considers the location of
 123 individual trees to be removed by thinning in evenly spaced rows. (c) considers even thinning on
 124 sloped terrain, and (d) represents variably spaced thinning on sloped terrain with more trees in
 125 valleys (lower thinning intensity) and fewer trees in ridge tops (higher thinning intensity).
 126 Dashed lines represent the water table.

127

128 Materials and methods

129 Model

130

131 In this study, we used ParFlow-TREES, an integrated ecohydrological model that couples a plant
 132 physiology model, Terrestrial Regional Ecosystem Exchange Simulator (TREES) [55], to a
 133 variably saturated groundwater model, PARallel FLOW (ParFlow) [56]. Briefly, ParFlow solves
 134 the three-dimensional, saturated and unsaturated subsurface flow using the mixed form of
 135 Richards' equation [57, 58], and has been extensively evaluated against observations of water
 136 table depth and streamflow across continental U.S. [59]. TREES simulates canopy
 137 photosynthesis and transpiration at 30-min time steps by explicitly solving for plant hydraulic
 138 transport and hydraulic-based stomatal optimization [60, 61]. TREES has been shown to reliably
 139 capture the responses of leaf water potential, transpiration, and photosynthesis to environmental
 140 cues of soil water, vapor pressure deficit, temperature, and CO₂ [20, 62, 63]. The integrated
 141 model, ParFlow-TREES, explicitly solves the transient water fluxes through the soil-plant-
 142 atmosphere continuum vertically and across the landscape laterally. It is therefore very suitable
 143 for investigating the impacts of topography and the spatial arrangement of trees on the ecosystem
 144 mortality risk and water and carbon fluxes. Descriptions of major processes of ParFlow-TREES
 145 are provided in Supporting Information Method S1 and previous literature [51, 52, 64].

146 Study area and model evaluation

147

148 We focused on a ponderosa pine (*Pinus ponderosa*) forest located in the Northern Arizona
 149 University Centennial Forest (35° 5' 20.5" N, 111° 45' 43.33" W) with an elevation of 2180 m
 150 above sea level. This is the Ameriflux site US-Fuf (<https://ameriflux.lbl.gov/sites/siteinfo/US-Fuf>).

151 Fuf) and observations of air temperature, precipitation, photosynthetically active radiation, wind
 152 speed, vapor pressure deficit (VPD), evapotranspiration (ET), and gross primary production
 153 (GPP) were collected during 2006-2010 at 30 min intervals. The data acquisition, processing and
 154 analysis have been described in previous publications [65, 66]. The mean annual temperature
 155 was 8.8 C° and the mean annual precipitation was 610 mm during the observation periods. The
 156 site typically experiences a bimodal precipitation pattern, with winter snowfall and rainfall
 157 occurring primarily in December through April, a pronounced drought during May and June and
 158 a rainy period associated with the North American Monsoon during July-September [65, 66].
 159 The soil is primarily clayloam and the forest is dominated by ponderosa pine with a very sparse
 160 understory of grasses and forbs. The measured leaf area index (LAI; projected area) was 2.2 m²
 161 m⁻², basal area was 30 m² ha⁻¹, and tree density was 853 trees ha⁻¹ [66, 67].

162 To ensure the model reliably captures the water and carbon fluxes, we evaluated the predictions
 163 of ParFlow-TREES against the observed evapotranspiration (ET) and gross primary production
 164 (GPP) within the tower footprint by simulating the entire forest stand in a lumped, one-
 165 dimensional mode. We focused on ET and GPP because of their critical role in the terrestrial
 166 water and carbon cycle [1, 68], and their wide usage in ecosystem model evaluations [69-71].
 167 Key model parameters of plant traits and soil properties were estimated based on previous
 168 literature as described in Table 1. Five years of meteorological conditions of air temperature,
 169 VPD, radiation, wind speed, and precipitation at 30-min time steps were used to run the
 170 simulation. Pearson's correlation (R) and Root Mean Square Error (RMSE) were calculated to
 171 quantify the agreement between model predictions and data observations of ET and GPP.

172 Table 1. Major inputs of ParFlow-TREES and associated values used in this study.

Model variable or parameter	Values	Sources
(a) Plant hydraulics parameters		
Weibull vulnerability curve parameter [b, c] ¹	[1.56, 1.41] for root [3.81, 2.5] for stem [2.08, 3.72] for leaf	[72]
Leaf-specific hydraulic conductance (LSC)	10 mmol s ⁻¹ m ⁻² MPa ⁻¹	[72]
Maximum carboxylation rate at 25 degree C (Vmax)	32 μmol m ⁻² s ⁻¹	[72]
Rooting depth	1.7 m	Assumed
Leaf area index	2.2 m ² m ⁻²	[65]
(b) Hydrologic parameters		
Number of vertical soil layers	10	Assumed
Thickness of soil layers (from top to bottom)	0.02, 0.1, 0.2, 0.2, 0.4, 0.8, 1.6, 3.2, 6.4, 7.1 (m)	Assumed
Van Genuchten parameters [a, n]	Clayloam [1.9, 1.31]	[65]
Saturated permeability	Clayloam [0.0026 m h ⁻¹]	[65]
Saturated soil moisture	0.450 m ³ m ⁻³	
Residual soil moisture	0.095 m ³ m ⁻³	
(c) Initial & boundary condition		

Boundary condition	No flow except for the surface allowing overland flow when the water table rises to the land surface
Initial condition	-10 m
(d) Spatial Setup	
Grid size	96 m*24 m for one dimension (lumped) simulation 1 m*1 m for three dimension (spatially explicit) simulation
Domain	1*1*10 for one dimension 96*24*10 for three dimension

¹⁷³ ¹ The vulnerability curve is characterized using Weibull function $f(\varphi) = e^{-(\frac{-\varphi}{b})^c}$, where φ is
¹⁷⁴ xylem pressure, and b and c are curve parameters.

¹⁷⁵

¹⁷⁶ Numerical experiments and hypothesis testing

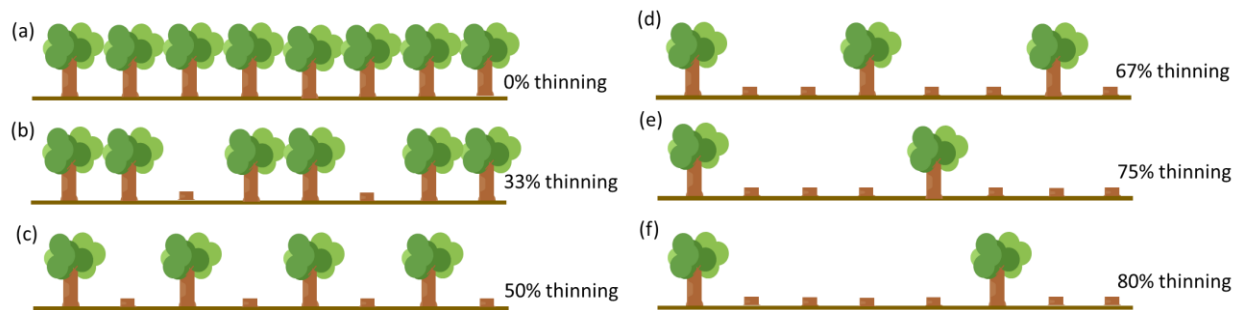
¹⁷⁷

¹⁷⁸ Using the evaluated model, we performed four sets of numerical experiments (Table 2) to
¹⁷⁹ investigate how topography and thinning interact to influence tree water use, carbon uptake, and
¹⁸⁰ mortality risk at individual tree and whole stand levels, across a range of climate conditions and
¹⁸¹ thinning intensities. We considered three different meteorological scenarios (Figure S1): a wet
¹⁸² year at the study area (2007) with annual precipitation of 653 mm, a dry year (2009) with annual
¹⁸³ precipitation of 296 mm, and an extreme dry year with the same weather variables as 2009
¹⁸⁴ except the precipitation was reduced by half (148 mm). Although the wet year had higher total
¹⁸⁵ precipitation, it had a long dry period before the onset of monsoon rains in late summer. We also
¹⁸⁶ considered six levels of thinning intensities, corresponding to 0%, 33%, 50%, 66%, 75%, and
¹⁸⁷ 80% of tree removal. Since this study focused on the impacts of tree spatial arrangement and
¹⁸⁸ topography, all trees were assumed to have the same traits (Table 1) and the grid cell became
¹⁸⁹ bare soil when trees were removed in spatially explicit simulations. For every simulation with
¹⁹⁰ different climate, thinning treatments, and topography, we reported the maximum percentage
¹⁹¹ loss of whole-plant hydraulic conductance (PLK), which has been used as an indicator of tree
¹⁹² mortality risk with higher PLK associated with higher mortality risk [20, 64]. We further
¹⁹³ reported the annual transpiration and productivity per leaf area (individual tree performance
¹⁹⁴ proxy) and per ground area for the entire forest stand (aggregated effect).

¹⁹⁵ In the first experiment, we ran one-dimensional simulations that reduced stand leaf area from 2.2
¹⁹⁶ to 1.46, 1.1, 0.73, 0.55, and 0.44 to represent different thinning intensities in a lumped mode
¹⁹⁷ (Figure 1a). This configuration mimicked the commonly adopted approaches by current
¹⁹⁸ ecosystem models that represent thinning through reduced leaf area index (LAI) at the stand
¹⁹⁹ scale. In the second to fourth experiments, we ran spatially explicit, three-dimensional
²⁰⁰ simulations with a model domain of 96 by 24 grid cells and a grid size of 1 m by 1 m. Every grid
²⁰¹ cell was covered by a ponderosa pine tree and evenly spaced row thinning was used to achieve
²⁰² different thinning intensities (Figure 2). For example, every third row was removed in 33%
²⁰³ thinning and every second row was removed in 50% thinning. Terrain was assumed to be flat in
²⁰⁴ the second experiment. To evaluate the influence of topography-induced lateral flow, we ran a
²⁰⁵ third experiment that simulated the forest stand on an idealized hillslope (Figure S2) and applied
²⁰⁶ the same thinning treatments as in Experiment 2.

207 Table 2. Descriptions of numerical experiments and how they were used to test hypotheses about
 208 explicit thinning, topography, and variable thinning.

Experiments	Description of the procedure	Hypothesis
Experiment 1 (3 climate scenarios * 6 thinning treatments for a total of 18 simulations)	1D model domain; vary leaf area index values from 2.2 to 1.46, 1.1, 0.73, 0.55, and 0.44.	Lumped thinning overestimates the benefits of water savings, compared to explicit thinning
Experiment 2 (3 climate scenarios * 6 thinning treatments for a total of 18 simulations)	3D model domain; vary the percentage of bare soil covered grid cells from 0% to 33%, 50%, 66%, 75%, and 80%. Evenly spaced row thinning was used to achieve a given thinning intensity. Terrain is flat	Lateral flow buffers tree stress on hillslopes, and impacts the effectiveness of thinning
Experiment 3 (3 climate scenarios * 6 thinning treatments for a total of 18 simulations)	Same as Experiment 2, except a sloped terrain is prescribed.	
Experiment 4 (3 climate scenarios * 1 variable thinning treatment for a total of 3 simulations)	Same as Experiment 3, except variably spaced row thinning was developed to minimize the total number of trees to be removed while keeping the mortality risk to the minimum or under 60%.	Variable thinning better reduces tree mortality risk and improves stand-scale productivity

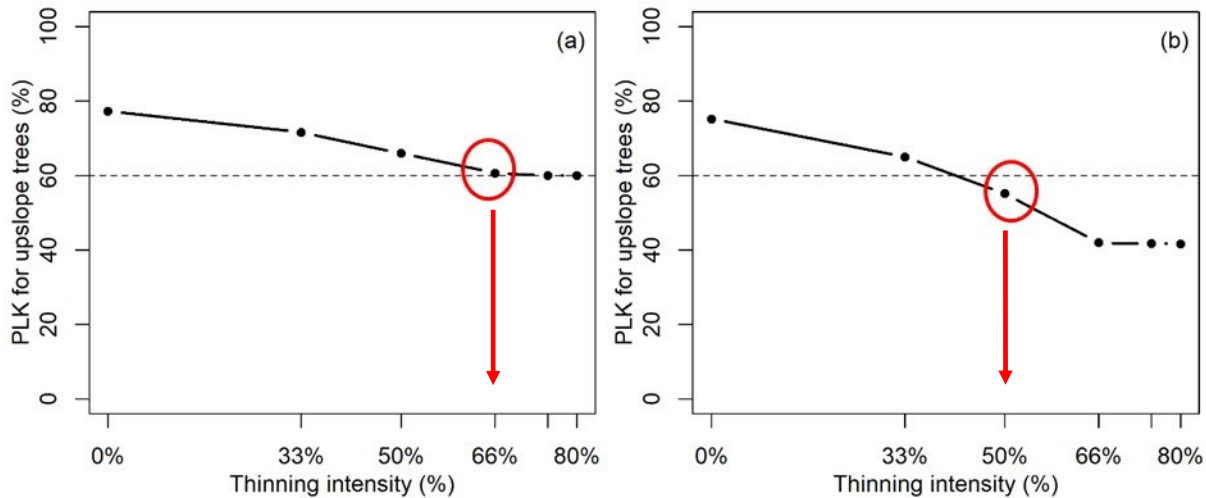


209

210 Figure 2. Diagram illustrating the evenly spaced thinning at different intensities with 0% thinning (a), 33% thinning (b, remove one of every three trees), 50% thinning (c, remove one of every two trees), 67% thinning (d, remove two of every three trees), 75% thinning (e, remove three of every four trees), and 80% thinning (f, remove four of every five trees).

211 In the fourth experiment, we simulated variable thinning that adjusts thinning intensity
 212 depending on the hillslope position to better take advantage of the laterally redistributed water.
 213 Based on simulations from Experiment 3, we plotted the mean PLK for upslope trees (distance in
 214 the uphill direction > 40 m) versus even thinning intensity (Figure 3). PLK kept declining as
 215 thinning intensity increased until a certain tipping point (red circles in Figure 3). This tipping
 216 point was used to determine the highest thinning intensity at upslope locations (Figure 3a). In
 217 some cases, PLK would drop below 60% before approaching the tipping point (Figure 3b), the

222 lowest thinning intensity that keeps PLK under 60% will be used. We used 60% loss in plant
 223 hydraulic conductance as the mortality threshold, informed by previous synthesis work showing
 224 60% best distinguishes trees that survived from those that died from droughts [15, 54]. For lower
 225 slope positions, the thinning intensity is determined by maintaining as many trees as possible
 226 while keeping the mortality risk of every individual tree under 60%. For example, 0% thinning
 227 will be applied in downslope locations where PLK is always under 60% due to lateral flow
 228 subsidy, and intermediate thinning intensities will be selected in the middle, transitional zone,
 229 accounting for the effects of both topography and neighboring tree distance.



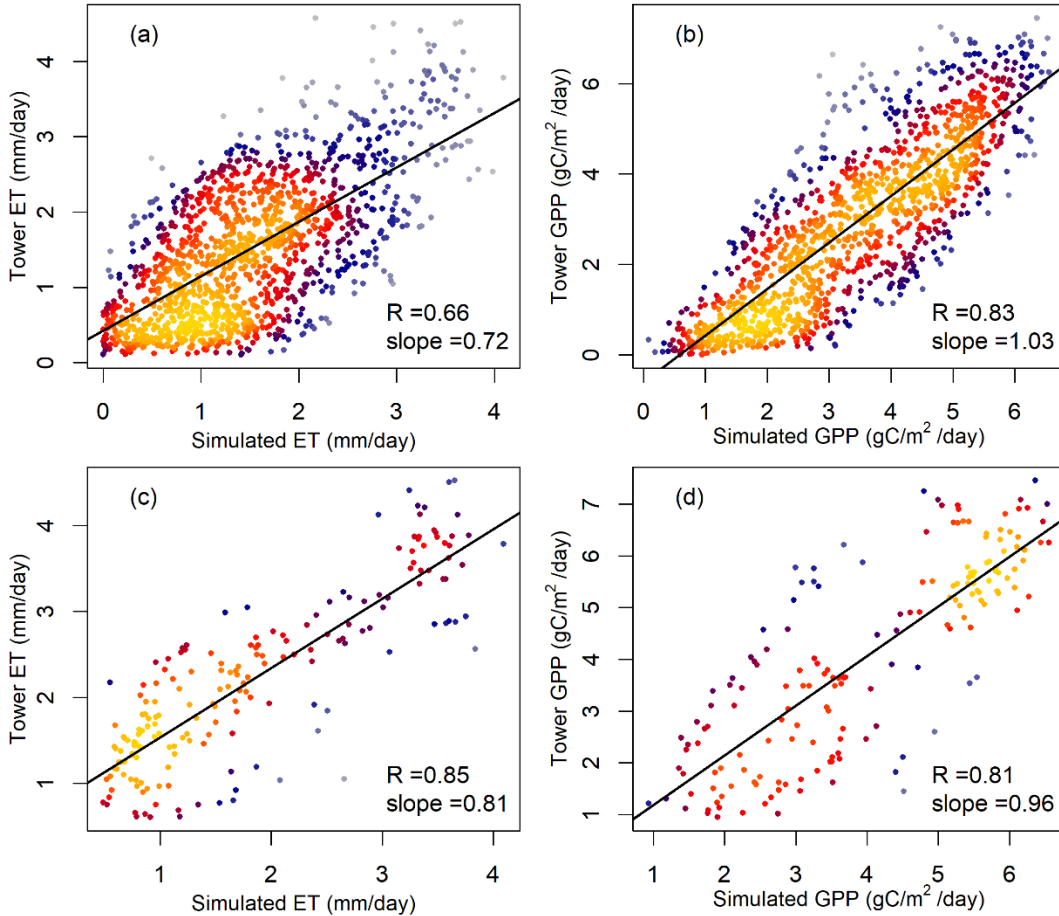
230

231 Figure 3. Changes in the PLK of upslope trees (Distance in the uphill direction > 40 m) versus
 232 thinning intensity. PLK generally declines as thinning intensity increases until a certain tipping
 233 point. If PLK levels off before reaching 60% PLK (a), the tipping point was used to determine
 234 the highest thinning intensity in upslope positions (66% thinning, highlighted by the red circle in
 235 a). If PLK levels off after reaching 60% PLK (b), the lowest thinning intensity that keeps PLK
 236 under 60% will be used (50% thinning, highlighted by the red circle in b).

237 Results

238 Model evaluation

239 A comparison between the observed and simulated daily values of ET and GPP showed that
 240 ParFlow-TREES reasonably captured the stand-scale responses of water and carbon fluxes
 241 during the five years from 2006 to 2010 (Figure 4, S3). Throughout the five years, the Pearson's
 242 correlation coefficient between observation and simulation was 0.66 for ET and 0.83 for GPP,
 243 and the regression slope between observed and predicted values was 0.72 for ET and 1.03 for
 244 GPP (Figure 4ab). For days when ET is likely dominated by transpiration such as growing
 245 season days without precipitation, the Pearson's correlation coefficient was 0.85 for ET and 0.81
 246 for GPP and the regression slope was 0.81 for ET and 0.96 for GPP.



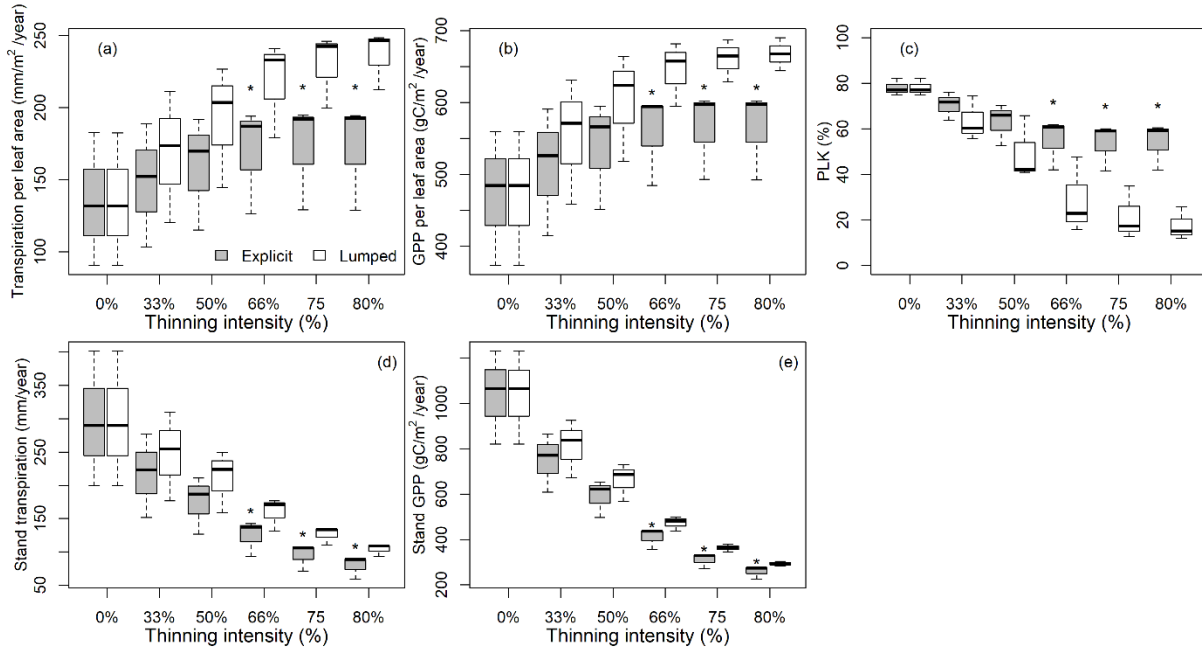
247

248 Figure 4. Scatter plot between ParFlow-TREES simulated and observed daily values of
 249 evapotranspiration (ET, a, c) and gross primary productivity (GPP, b, d) from an eddy covariance
 250 flux tower at an Ameriflux Site US-FUF, in a ponderosa pine forest near Flagstaff, Arizona
 251 during the period of 2006 to 2010. a and b include data points for the entire five year period. c
 252 and d only include days when ET is likely dominated by transpiration, determined as days during
 253 the growing season from June to August and had no precipitation. Warmer dot colors indicate a
 254 higher point density, and the black lines indicate the linear regression fit. R is the Pearson's
 255 correlation coefficient and slope is the regression slope between observed and modeled values.
 256

257 Lumped versus spatially explicit representation of stand thinning

258 We compared the transpiration, productivity, and mortality risks of the remaining trees using
 259 model representations of lumped (Experiment 1) versus explicit tree removal (Experiment 2)
 260 across different thinning intensities and climate scenarios (Figure 5, S4). Reducing tree densities
 261 generally improved transpiration and productivity per leaf area, for both lumped and explicit
 262 thinning (Figure 5ab). While lumped and spatially explicit simulations had the same transpiration
 263 and productivity with 0% thinning, their discrepancies increased with thinning intensity (gray
 264 versus white bars in Figure 5), and was significant at a thinning intensity of 66% ($p < 0.1$).
 265 Lumped thinning tended to overestimate water savings from thinning, with higher increases in
 266 transpiration and productivity per unit leaf area and reductions in PLK. Further, lumped thinning
 267 predicted continued decrease in PLK with thinning intensity, whereas spatially explicit thinning

268 predicted PLK to level off at intensities of 66%. Finally, increased transpiration and productivity
 269 at leaf-scale was not sufficient to compensate for tree removal at stand scale, leading to
 270 decreased transpiration and productivity of the entire stand (Figure 5de).

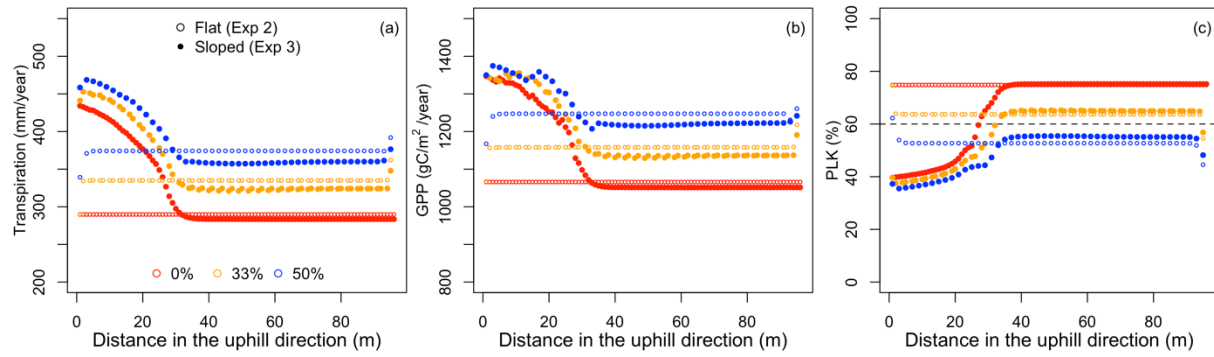


271

272 Figure 5. Boxplots of transpiration per unit leaf area (a), productivity (GPP) per unit leaf area
 273 (b), maximum percentage loss of whole-plant hydraulic conductance (PLK) (c), stand
 274 transpiration per ground area (d), and stand GPP per ground area (e) across different thinning
 275 intensities of 0%, 33%, 50%, 66%, 75%, and 80%, using lumped (white bars, Experiment 1)
 276 versus explicit (grey bars, Experiment 2) representations of tree removal. For explicit
 277 simulations, only mean values are presented in a-c. Stars represent significant ($p < 0.1$)
 278 differences between lumped and explicit simulations based on t test.
 279

280 Forest thinning on flat versus sloped terrains

281 We compared forest responses to explicit thinning at even distances between flat (Experiment 2)
 282 and sloped terrains (Experiment 3). Trees on the flat terrain showed little spatial variation,
 283 whereas trees on the hillslope demonstrated large spatial gradients in PLK, transpiration, and
 284 productivity (Figure 6, S5-S7). As soil water laterally redistributed from topographic high to low,
 285 trees on the lower hillslope received additional water subsidy, and therefore had higher
 286 transpiration and productivity and lower PLK (Figure 6, uphill distance < 30 m). Trees on the dry
 287 upslopes had lower transpiration, productivity and higher PLK (Figure 6, uphill distance > 30
 288 m). Averaged across the stand, transpiration and productivity were higher and PLK was lower
 289 for forests on hillslopes, compared to flat terrains (Figure S8-S10). Further, the differences
 290 between flat and sloped forest stands were greater at lower thinning intensities (greater forest
 291 density) when the total demand for water was higher.

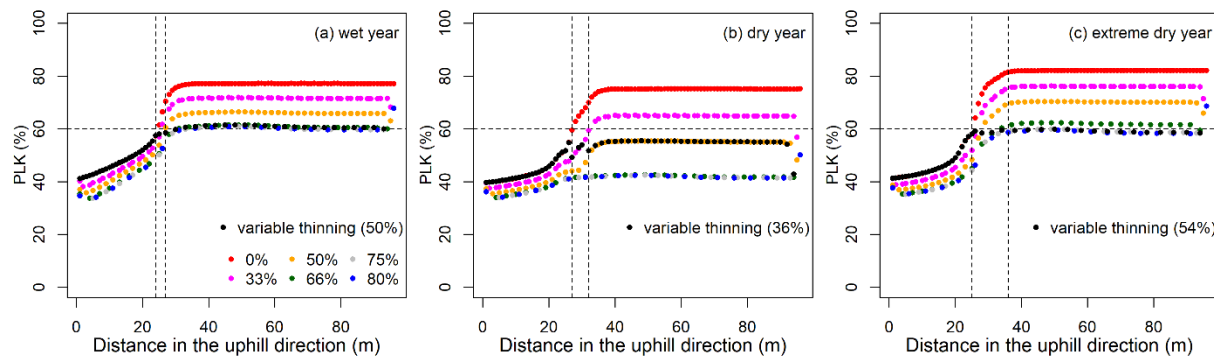


292

293 Figure 6. Spatial variations in transpiration (a), productivity (GPP, b), and mortality risk (PLK,
 294 c) along the uphill direction of a forested stand during the dry year and for different terrains with
 295 solid dots representing sloped terrain (Experiment 3) and open dots representing flat terrain
 296 (Experiment 2). Every dot represents a grid cell that has tree coverage. Only three thinning
 297 intensities were shown for easier visualization (red: 0%, orange: 33%, and blue 50%).

298 Variable thinning effects on ecosystem responses

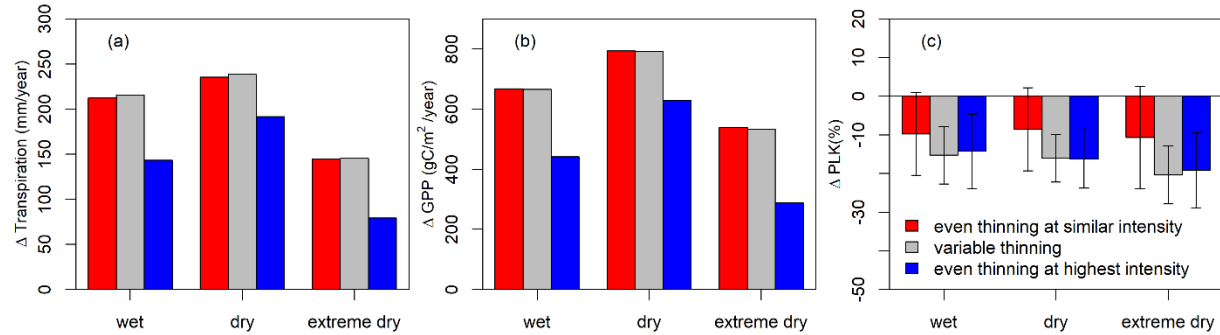
299 We developed a variable thinning strategy (Experiment 4) that adjusted thinning intensity (or
 300 inter-tree spacing) based on hillslope positions and climate conditions (Figure 7, black versus
 301 colored dots). Compared to even thinning, variable thinning achieved lower PLK for upslope
 302 trees (Figure 7ac), except for the dry year where 50% thinning was selected as the PLK for
 303 upslope trees was lower than 60% (Figure 7b). Further, variable thinning maintained more trees
 304 in the lower hillslope to better utilize the water subsidy at hillslope bottoms through lateral
 305 subsurface flow while keeping PLK less than 60%. At the whole stand scale, variable thinning
 306 resulted a thinning intensity of 50% for the wet year, 36% for the dry year, and 54% for the
 307 extreme dry year. Compared to even thinning at similar intensities, variable thinning had similar
 308 stand transpiration and productivity but more mitigated PLK (Figure 8, red versus grey bars).
 309 Compared to even thinning at the highest intensity of variable thinning (66% for wet year, 50%
 310 for dry year, and 75% for extremely dry year), variable thinning had similar reduction in PLK,
 311 but higher stand transpiration and productivity by maintaining more trees (Figure 8, blue versus
 312 grey bars).



313

314 Figure 7. Variations in individual tree mortality risk (PLK) along the uphill direction of a
 315 hypothetical hillslope, for even thinning at various intensities (different colors) and variable
 316 thinning (black), during wet (a), dry (b), and extreme dry (c) years. Every dot represents an

317 individual model grid with tree coverage. Numbers in the parentheses indicate the stand-scale
 318 thinning intensity. Dashed lines represented 60% mortality risk threshold (horizontal) and the
 319 location to change thinning intensities (vertical).



320
 321 Figure 8. Changes in stand transpiration (ΔT , a), productivity (ΔGPP , b) and mortality risk
 322 (ΔPLK , c) from variable thinning (grey bars), even thinning at similar intensities (red bars), and
 323 highest intensities (blue bars), across different years. Variable thinning intensity was 50% for
 324 wet year, 35% for dry year, and 54% for extremely dry year. Even thinning at similar intensity
 325 was 50% for wet year, 33% for dry year, and 50% for extremely dry year. Even thinning at
 326 upslope intensity was 66% for wet year, 50% for dry year, and 75% for extremely dry year. 0%
 327 thinning on sloped terrains was used as the baseline to calculate the changes. Error bars in c
 328 represented the standard deviation among trees within the forest stand.

329 Discussion

330 Developing effective strategies that mitigate forest vulnerability to drought has become a major
 331 research frontier to inform forest management [6, 12, 36, 73]. In this study, we evaluated the
 332 sensitivity of forest functions and mortality risks to within-stand variations of tree arrangement
 333 and topography using a coupled plant hydraulics-hydrology model, across thinning intensities
 334 and over highly variable climate. Our results showed that the explicit consideration of water
 335 transport among neighboring trees and along hillslope within a forest stand strongly influence the
 336 estimated effectiveness of thinning in reducing water stress and mortality risk to drought.
 337 Further, topography could be leveraged to develop variable thinning treatments that can enhance
 338 both stand productivity and individual level resistance against drought stress. Our numerical
 339 experiments highlighted the need for an explicit consideration of within-stand heterogeneity in
 340 trees and abiotic environment when designing mitigation strategies.

341 The spatially explicit simulation of individual tree removal was compared with the lumped
 342 reduction in stand leaf area that is commonly employed in process-based ecosystem models [38,
 343 39]. Our results showed the lumped thinning tended to overestimate the amount of water savings
 344 for a given thinning intensity (Figure 5). This discrepancy was primarily because water saved by
 345 thinning became immediately available to the remaining biomass in the lumped reduction in leaf
 346 area, whereas in a spatially explicit manner, water would have to laterally transport from inter-
 347 tree spaces into tree locations before the extra water could subsidize the neighboring tree.
 348 Further, the extra water could be consumed by increased evapotranspiration from bare soil or
 349 understory after overstory tree removal [74, 75]. As thinning intensity increases, spatially
 350 explicit thinning suggested minimal changes in transpiration, productivity, and mortality risk
 351 beyond a certain point, whereas lumped thinning suggested continued increases in transpiration

352 and productivity and decreases in mortality risk as more biomass was being removed (Figure 5a-
353 c).

354 By explicitly solving plant hydraulics for each individual tree within the stand, our results
355 showed that thinning improved leaf-level gas exchanges and reduced PLK to drought (Figure 5a-
356 c), while the stand-scale productivity and transpiration decreased due to the removal of trees
357 (Figure 5d, e). These results are consistent with earlier leaf-level observations from nearby sites
358 [65, 76, 77] and stand-scale estimations from other places [26, 50]. Further, thinning was more
359 effective to decrease mortality risk when drought was mild such as the dry year, and less
360 effective when total precipitation was very low (e.g., extreme dry year) or when there was a long
361 drought period (e.g., the wet year, Figure S1). Overall, our results support the view that density
362 management has the potential to compensate for the deleterious effects of drought and to
363 promote resilience to drier future climates [12, 28] and that management strategies need to be
364 tailored to specific local context and environmental conditions [6].

365 By simulating forest stands on a sloped terrain, our study showed topography creates fine-scale
366 spatial heterogeneities of plant responses within the same forest stand through lateral
367 groundwater flow (Figure 6, S5-7). While topography is generally recognized in empirical
368 studies [78-80], topography-mediated water supply is more rarely considered in ecosystem
369 models (but see [52, 81]) or incorporated into forest management design. Trees in lower
370 topographic positions received the water subsidy via lateral flow from higher positions at the cost
371 of reducing water supply for trees at higher topographic positions (Figure 6). But the stand-scale
372 productivity and transpiration were higher and mortality risk was lower compared to forests on
373 flat terrains (Figure S8-10), suggesting a net benefit of lateral water redistribution at the stand
374 scale [41]. Further, the differences between flat and sloped terrains increased with water stress
375 when stand density is high or climate condition is dry (Figure S8-10). This result was in line with
376 previous studies suggesting complexities in topography complicated the prediction of forest
377 mortality from climate variables [22, 46].
378

379 Based on the changes of PLK to various even thinning intensities, a variable thinning scheme
380 (Figure 3) was developed to demonstrate how sloped terrain might be incorporated into forest
381 treatment design. Our results demonstrated topographically-informed variable thinning could
382 lead to higher stand productivity and lower mortality risk compared to even thinning (Figure 8).
383 Keeping more trees in lower hillslope positions took better advantage of the extra water made
384 available through groundwater redistribution, whereas increasing inter-tree distance in the dry
385 upslope helped to release water stress (Figure 7). Variable thinning requires solving for water
386 dynamics that are modulated by climate, tree neighborhood, and topography. This dynamic
387 response cannot be predetermined, and can only be captured by models solving transient water
388 fluxes through soil-plant atmosphere continuum and across the landscape, such as ParFlow-
389 TREES [51]. Previous research on variable thinning focused on the creation of structurally
390 complex stands by creating different gap sizes, age or species compositions [28, 82]. Our work
391 adds to this body of literature by providing a paradigm to incorporate terrain into forest
392 management and predictive models [50].
393

394 While this study illustrated the potential influence of tree arrangements and topography in
395 affecting forest health, there were several caveats that are worth further investigations. First, this
396 study was based on idealized experiments with hypothetical terrain and density treatments.

397 Future work should combine numerical modeling with more realistic and detailed topography
398 and pre- and post-treatment forest structure and incorporate the differences in plant functional
399 traits associated with variations in tree size, age, and species that are important for modulating
400 ecosystem responses [83, 84]. Second, we relied on the eddy covariance measurements of
401 ecosystem water and carbon fluxes to evaluate model performance. Although this approach has
402 been commonly used [69-71], it does not explicitly consider the separate water fluxes of
403 transpiration, soil evaporation, and canopy evaporation. Long-term, simultaneous, and accurate
404 measurements of these water balance components and their dynamics following thinning
405 treatments will be critical to better constrain model uncertainty [85]. Similarly, additional
406 processes that modify the water dynamics and microclimate such as radiation, temperature and
407 vapor pressure deficit might be equally important [26, 86, 87] and should be incorporated to
408 comprehensively understand the impacts of thinning on forest functions. Third, we used the
409 maximum percentage loss of hydraulic conductivity as a proxy of drought-induced mortality
410 risk. While this metric has been successful in predicting several episodes of mortality [18, 54,
411 64], future work should evaluate its potential in explaining observed tree mortality across sites
412 with and without treatments. Finally, while this study focused on short-term changes in water
413 and carbon fluxes and drought mortality risks after thinning, dynamics of forest composition and
414 structure after thinning treatments might influence ecosystem resilience to drought and other
415 compounded disturbances in the long term [88-90].

416 **Conclusion**

417 Developing effective adaptation strategies to changing climate hinges on an adequate
418 understanding of the mechanisms governing drought vulnerability of forests. Using a coupled
419 plant hydraulics-hydrology model, this study quantified the effects of within-stand variations in
420 tree arrangement and topography on ecosystem functions and mortality risks and demonstrated
421 the potential of ecohydrological models to estimate forest vulnerability to climate change under
422 alternative management scenarios. Our results suggested inter-tree spacing and topography could
423 strongly modulate ecosystem functions and mortality risks at individual tree and stand scales.
424 Further, variable thinning that adjusts tree densities with topography could result in enhanced
425 forest functions and health. These findings provide mechanistic evidence that density
426 management has the potential to compensate for the deleterious effects of drought. They also
427 underscore the important interaction between tree location and terrain in mediating drought-
428 related mortality risk, and thus should be incorporated when designing forest management
429 strategies.

430

431 **Acknowledgements**

432 X.T. acknowledges funding from National Science Foundation (NSF) Grant DEB 2106030 and
433 Department of Energy (DOE) DE-SC0023308. M.D.V. was supported by Grant RYC2020-
434 029792-I funded by MCIN/AEI/ 10.13039/501100011033 and by “ESF Investing in your
435 future”. The statements made in this manuscript reflect the views of the authors and do not
436 necessarily reflect the views of the funding agencies. USDA is an equal-opportunity employer.

437 **Data availability statement**

438 The eddy covariance flux data can be accessed from <https://ameriflux.lbl.gov/sites/siteinfo/US-Fuf>. The model experiment results that support the findings of this study are available upon
439 request from the authors.

441

442 **References**

- 443 1. Bonan, G.B., *Forests and climate change: forcings, feedbacks, and the climate benefits of*
444 *forests*. *science*, 2008. **320**(5882): p. 1444-1449.
- 445 2. Mori, A.S., K.P. Lertzman, and L. Gustafsson, *Biodiversity and ecosystem services in*
446 *forest ecosystems: a research agenda for applied forest ecology*. *Journal of Applied*
447 *Ecology*, 2017. **54**(1): p. 12-27.
- 448 3. Allen, C.D., D.D. Breshears, and N.G. McDowell, *On underestimation of global*
449 *vulnerability to tree mortality and forest die-off from hotter drought in the Anthropocene*.
450 *Ecosphere*, 2015. **6**(8): p. 1-55.
- 451 4. Abatzoglou, J.T. and A.P. Williams, *Impact of anthropogenic climate change on wildfire*
452 *across western US forests*. *Proceedings of the National Academy of Sciences*, 2016.
453 **113**(42): p. 11770-11775.
- 454 5. Raffa, K.F., et al., *Cross-scale drivers of natural disturbances prone to anthropogenic*
455 *amplification: the dynamics of bark beetle eruptions*. *Bioscience*, 2008. **58**(6): p. 501-517.
- 456 6. Grant, G.E., C.L. Tague, and C.D. Allen, *Watering the forest for the trees: an emerging*
457 *priority for managing water in forest landscapes*. *Frontiers in Ecology and the*
458 *Environment*, 2013. **11**(6): p. 314-321.
- 459 7. Zhang, F., et al., *Five decades of observed daily precipitation reveal longer and more*
460 *variable drought events across much of the western United States*. *Geophysical Research*
461 *Letters*, 2021. **48**(7): p. e2020GL092293.
- 462 8. Choat, B., et al., *Triggers of tree mortality under drought*. *Nature*, 2018. **558**(7711): p. 531-
463 539.
- 464 9. Dai, A., *Increasing drought under global warming in observations and models*. *Nature*
465 *climate change*, 2013. **3**(1): p. 52-58.
- 466 10. IPCC, *Climate Change 2023: Synthesis Report. Contribution of Working Groups I, II and*
467 *III to the Sixth Assessment Report of the Intergovernmental Panel on Climate Change*
468 *2023*: Geneva, Switzerland.
- 469 11. Anderegg, W.R., J.M. Kane, and L.D. Anderegg, *Consequences of widespread tree*
470 *mortality triggered by drought and temperature stress*. *Nature Climate Change*, 2013. **3**(1):
471 p. 30-36.
- 472 12. Furniss, T.J., et al., *Crowding, climate, and the case for social distancing among trees*.
473 *Ecological Applications*, 2022. **32**(2): p. e2507.
- 474 13. Bottero, A., et al., *Density-dependent vulnerability of forest ecosystems to drought*. *Journal*
475 *of Applied Ecology*, 2017. **54**(6): p. 1605-1614.
- 476 14. Grossiord, C., *Having the right neighbors: how tree species diversity modulates drought*
477 *impacts on forests*. *New Phytologist*, 2020. **228**(1): p. 42-49.
- 478 15. Sperry, J.S. and D.M. Love, *What plant hydraulics can tell us about responses to climate-*
479 *change droughts*. *New Phytologist*, 2015. **207**(1): p. 14-27.

- 480 16. McDowell, N.G., et al., *Mechanisms of woody-plant mortality under rising drought, CO₂*
481 and vapour pressure deficit
482. *Nature Reviews Earth & Environment*, 2022. **3**(5): p. 294-308.
- 483 17. Sperry, J.S. and M.T. Tyree, *Mechanism of water stress-induced xylem embolism*. *Plant*
484 *physiology*, 1988. **88**(3): p. 581-587.
- 485 18. McDowell, N.G., et al., *Evaluating theories of drought-induced vegetation mortality using*
486 *a multimodel-experiment framework*. *New Phytologist*, 2013. **200**(2): p. 304-321.
- 487 19. Johnson, D.M., et al., *Co-occurring woody species have diverse hydraulic strategies and*
488 *mortality rates during an extreme drought*. *Plant, cell & environment*, 2018.
- 489 20. Venturas, M.D., et al., *A stomatal control model based on optimization of carbon gain*
490 *versus hydraulic risk predicts aspen sapling responses to drought*. *New Phytologist*, 2018.
491 **220**(3): p. 836-850.
- 492 21. Trugman, A.T., et al., *Why is tree drought mortality so hard to predict?* *Trends in Ecology*
493 & *Evolution*, 2021. **36**(6): p. 520-532.
- 494 22. Venturas, M.D., et al., *Understanding and predicting forest mortality in the western United*
495 *States using long-term forest inventory data and modeled hydraulic damage*. *New*
496 *Phytologist*, 2021. **230**(5): p. 1896-1910.
- 497 23. Clark, J.S., et al., *Competition-interaction landscapes for the joint response of forests to*
498 *climate change*. *Global Change Biology*, 2014. **20**(6): p. 1979-1991.
- 499 24. Van Mantgem, P.J., et al., *Pre-fire drought and competition mediate post-fire conifer*
500 *mortality in western US National Parks*. *Ecological applications*, 2018. **28**(7): p. 1730-
501 1739.
- 502 25. Boyden, S., et al., *Seeing the forest for the heterogeneous trees: stand-scale resource*
503 *distributions emerge from tree-scale structure*. *Ecological Applications*, 2012. **22**(5): p.
504 1578-1588.
- 505 26. Tsamir, M., et al., *Stand density effects on carbon and water fluxes in a semi-arid forest,*
506 *from leaf to stand-scale*. *Forest Ecology and Management*, 2019. **453**: p. 117573.
- 507 27. Hood, S.M., S. Baker, and A. Sala, *Fortifying the forest: thinning and burning increase*
508 *resistance to a bark beetle outbreak and promote forest resilience*. *Ecological*
509 *Applications*, 2016. **26**(7): p. 1984-2000.
- 510 28. Knapp, E.E., et al., *Variable thinning and prescribed fire influence tree mortality and*
511 *growth during and after a severe drought*. *Forest Ecology and Management*, 2021. **479**: p.
512 118595.
- 513 29. Restaino, C., et al., *Forest structure and climate mediate drought-induced tree mortality in*
514 *forests of the Sierra Nevada, USA*. *Ecological Applications*, 2019. **29**(4): p. e01902.
- 515 30. Stephens, S.L., et al., *Forest restoration and fuels reduction: Convergent or divergent?*
516 *Bioscience*, 2021. **71**(1): p. 85-101.
- 517 31. Bradford, J.B. and D.M. Bell, *A window of opportunity for climate-change adaptation:*
518 *easing tree mortality by reducing forest basal area*. *Frontiers in Ecology and the*
519 *Environment*, 2017. **15**(1): p. 11-17.
- 520 32. Young, D.J., et al., *Long-term climate and competition explain forest mortality patterns*
521 *under extreme drought*. *Ecology letters*, 2017. **20**(1): p. 78-86.
- 522 33. Zhang, J., S. Huang, and F. He, *Half-century evidence from western Canada shows forest*
523 *dynamics are primarily driven by competition followed by climate*. *Proceedings of the*
524 *National Academy of Sciences*, 2015. **112**(13): p. 4009-4014.

- 525 34. Tai, X., A.T. Trugman, and W.R. Anderegg, *Linking remotely sensed ecosystem resilience*
526 *with forest mortality across the continental United States*. Global Change Biology, 2023.
527 **29**(4): p. 1096-1105.
- 528 35. Clark, J.S., et al., *The impacts of increasing drought on forest dynamics, structure, and*
529 *biodiversity in the United States*. Global change biology, 2016. **22**(7): p. 2329-2352.
- 530 36. Sohn, J.A., S. Saha, and J. Bauhus, *Potential of forest thinning to mitigate drought stress:*
531 *A meta-analysis*. Forest Ecology and Management, 2016. **380**: p. 261-273.
- 532 37. Dwivedi, R., et al., *Forest density and snowpack stability regulate root zone water stress*
533 *and percolation differently at two sites with contrasting ephemeral vs. stable seasonal*
534 *snowpacks*. Journal of Hydrology, 2023. **624**: p. 129915.
- 535 38. Bellassen, V., et al., *Modelling forest management within a global vegetation model—Part*
536 *1: Model structure and general behaviour*. Ecological Modelling, 2010. **221**(20): p. 2458-
537 2474.
- 538 39. Lindeskog, M., et al., *Accounting for forest management in the estimation of forest carbon*
539 *balance using the dynamic vegetation model LPJ-GUESS (v4. 0, r9710): implementation*
540 *and evaluation of simulations for Europe*. Geoscientific Model Development, 2021.
541 **14**(10): p. 6071-6112.
- 542 40. Sun, G., P.V. Caldwell, and S.G. McNulty, *Modelling the potential role of forest thinning*
543 *in maintaining water supplies under a changing climate across the conterminous United*
544 *States*. Hydrological Processes, 2015. **29**(24): p. 5016-5030.
- 545 41. Fan, Y., et al., *Hillslope Hydrology in Global Change Research and Earth System*
546 *Modeling*. Water Resources Research, 2019. **55**(2): p. 1737-1772.
- 547 42. Fan, Y., *Groundwater in the Earth's critical zone: Relevance to large-scale patterns and*
548 *processes*. Water Resources Research, 2015. **51**(5): p. 3052-3069.
- 549 43. Swetnam, T.L., et al., *Topographically driven differences in energy and water constrain*
550 *climatic control on forest carbon sequestration*. Ecosphere, 2017. **8**(4).
- 551 44. Hwang, T., et al., *Ecosystem processes at the watershed scale: Hydrologic vegetation*
552 *gradient as an indicator for lateral hydrologic connectivity of headwater catchments*.
553 Water Resources Research, 2012. **48**(6).
- 554 45. Tai, X., et al., *Hillslope hydrology influences the spatial and temporal patterns of remotely*
555 *sensed ecosystem productivity*. Water Resources Research, 2020. **56**(11): p.
556 e2020WR027630.
- 557 46. Tai, X., et al., *Plant hydraulics improves and topography mediates prediction of aspen*
558 *mortality in southwestern USA*. New Phytologist, 2017. **213**(1): p. 113-127.
- 559 47. Schwantes, A.M., et al., *Accounting for landscape heterogeneity improves spatial*
560 *predictions of tree vulnerability to drought*. New Phytologist, 2018. **220**(1): p. 132-146.
- 561 48. Price, M.F., *Why mountain forests are important*. The Forestry Chronicle, 2003. **79**(2): p.
562 219-222.
- 563 49. Fisher, R.A. and C.D. Koven, *Perspectives on the future of Land Surface Models and the*
564 *challenges of representing complex terrestrial systems*. Journal of Advances in Modeling
565 Earth Systems, 2020. **12**(4): p. e2018MS001453.
- 566 50. Tague, C.L. and M.A. Moritz, *Plant accessible water storage capacity and tree-scale root*
567 *interactions determine how forest density reductions alter forest water use and*
568 *productivity*. Frontiers in Forests and Global Change, 2019: p. 36.
- 569 51. Tai, X., et al., *Lateral subsurface flow modulates forest mortality risk to future climate and*
570 *elevated CO₂*. Environmental Research Letters, 2021. **16**(8): p. 084015.

- 571 52. Tai, X., et al., *Distributed Plant Hydraulic and Hydrological Modeling to Understand the*
572 *Susceptibility of Riparian Woodland Trees to Drought-Induced Mortality*. Water
573 Resources Research, 2018.
- 574 53. Hammond, W.M., et al., *Dead or dying? Quantifying the point of no return from hydraulic*
575 *failure in drought-induced tree mortality*. New Phytologist, 2019. **223**(4): p. 1834-1843.
- 576 54. Adams, H.D., et al., *A multi-species synthesis of physiological mechanisms in drought-*
577 *induced tree mortality*. Nature ecology & evolution, 2017. **1**(9): p. 1285.
- 578 55. Mackay, D.S., et al., *Interdependence of chronic hydraulic dysfunction and canopy*
579 *processes can improve integrated models of tree response to drought*. Water Resources
580 Research, 2015. **51**(8): p. 6156-6176.
- 581 56. Maxwell, R.M. and S.J. Kollet, *Interdependence of groundwater dynamics and land-*
582 *energy feedbacks under climate change*. Nature Geoscience, 2008. **1**(10): p. 665-669.
- 583 57. Maxwell, R.M., L. Condon, and S. Kollet, *A high-resolution simulation of groundwater*
584 *and surface water over most of the continental US with the integrated hydrologic model*
585 *ParFlow v3*. Geoscientific Model Development, 2015. **8**: p. 923-937.
- 586 58. Maxwell, R.M., et al., *ParFlow User's Manual*. 2016.
- 587 59. Yang, C., et al., *A high-resolution, 3D groundwater-surface water simulation of the*
588 *contiguous US: Advances in the integrated ParFlow CONUS 2.0 modeling platform*.
589 Journal of Hydrology, 2023. **626**: p. 130294.
- 590 60. Sperry, J.S., et al., *Pragmatic hydraulic theory predicts stomatal responses to climatic*
591 *water deficits*. New Phytologist, 2016.
- 592 61. Sperry, J.S., et al., *Predicting stomatal responses to the environment from the optimization*
593 *of photosynthetic gain and hydraulic cost*. Plant, cell & environment, 2017. **40**(6): p. 816-
594 830.
- 595 62. Wang, Y., et al., *The stomatal response to rising CO₂ concentration and drought is*
596 *predicted by a hydraulic trait-based optimization model*. Tree physiology, 2019. **39**(8): p.
597 1416-1427.
- 598 63. Love, D., et al., *Dependence of Aspen Stands on a Subsurface Water Subsidy: Implications*
599 *for Climate Change Impacts*. Water Resources Research, 2018.
- 600 64. Tai, X., et al., *Plant hydraulic stress explained tree mortality and tree size explained beetle*
601 *attack in a mixed conifer forest*. Journal of Geophysical Research: Biogeosciences, 2019.
- 602 65. Dore, S., et al., *Recovery of ponderosa pine ecosystem carbon and water fluxes from*
603 *thinning and stand-replacing fire*. Global change biology, 2012. **18**(10): p. 3171-3185.
- 604 66. Dore, S., et al., *Long-term impact of a stand-replacing fire on ecosystem CO₂ exchange of*
605 *a Ponderosa pine forest*. Global Change Biology, 2008. **14**(8): p. 1801-1820.
- 606 67. Dore, S., et al., *Carbon and water fluxes from ponderosa pine forests disturbed by wildfire*
607 *and thinning*. Ecological Applications, 2010. **20**(3): p. 663-683.
- 608 68. Yang, Y., et al., *Evapotranspiration on a greening Earth*. Nature Reviews Earth &
609 Environment, 2023. **4**(9): p. 626-641.
- 610 69. MacBean, N., et al., *Testing water fluxes and storage from two hydrology configurations*
611 *within the ORCHIDEE land surface model across US semi-arid sites*. Hydrology and Earth
612 System Sciences, 2020. **24**(11): p. 5203-5230.
- 613 70. Sabot, M.E.B., et al., *Plant profit maximization improves predictions of European forest*
614 *responses to drought*. New Phytologist, 2020. **226**(6): p. 1638-1655.

- 615 71. Eller, C.B., et al., *Stomatal optimization based on xylem hydraulics (SOX) improves land*
616 *surface model simulation of vegetation responses to climate.* *New Phytologist*, 2020.
617 **226**(6): p. 1622-1637.
- 618 72. Sperry, J.S., et al., *The impact of rising CO₂ and acclimation on the response of US forests*
619 *to global warming.* *Proceedings of the National Academy of Sciences*, 2019. **116**(51): p.
620 25734-25744.
- 621 73. Churchill, D.J., et al., *Restoring forest resilience: from reference spatial patterns to*
622 *silvicultural prescriptions and monitoring.* *Forest Ecology and Management*, 2013. **291**: p.
623 442-457.
- 624 74. Simonin, K., et al., *The influence of thinning on components of stand water balance in a*
625 *ponderosa pine forest stand during and after extreme drought.* *Agricultural and Forest*
626 *Meteorology*, 2007. **143**(3-4): p. 266-276.
- 627 75. Raz-Yaseef, N., E. Rotenberg, and D. Yakir, *Effects of spatial variations in soil*
628 *evaporation caused by tree shading on water flux partitioning in a semi-arid pine forest.*
629 *Agricultural and Forest Meteorology*, 2010. **150**(3): p. 454-462.
- 630 76. Feeney, S.R., et al., *Influence of thinning and burning restoration treatments on*
631 *presettlement ponderosa pines at the Gus Pearson Natural Area.* *Canadian Journal of*
632 *Forest Research*, 1998. **28**(9): p. 1295-1306.
- 633 77. McDowell, N.G., et al., *Homeostatic maintenance of ponderosa pine gas exchange in*
634 *response to stand density changes.* *Ecological Applications*, 2006. **16**(3): p. 1164-1182.
- 635 78. Gutierrez Lopez, J., et al., *How tree species, tree size, and topographical location*
636 *influenced tree transpiration in northern boreal forests during the historic 2018 drought.*
637 *Global change biology*, 2021. **27**(13): p. 3066-3078.
- 638 79. Fortunel, C., et al., *Topography and neighborhood crowding can interact to shape species*
639 *growth and distribution in a diverse Amazonian forest.* *Ecology*, 2018. **99**(10): p. 2272-
640 2283.
- 641 80. Brum, M., et al., *Hydrological niche segregation defines forest structure and drought*
642 *tolerance strategies in a seasonal Amazon forest.* *Journal of Ecology*, 2019. **107**(1): p. 318-
643 333.
- 644 81. Tague, C.L. and L. Band, *RHESSys: regional hydro-ecologic simulation system-an object-*
645 *oriented approach to spatially distributed modeling of carbon, water, and nutrient cycling.*
646 *Earth Interactions*, 2004. **8**(19): p. 1-42.
- 647 82. Puettmann, K.J., et al., *Forest restoration using variable density thinning: Lessons from*
648 *Douglas-fir stands in western Oregon.* *Forests*, 2016. **7**(12): p. 310.
- 649 83. McDowell, N.G., J. Licata, and B.J. Bond, *Environmental sensitivity of gas exchange in*
650 *different-sized trees.* *Oecologia*, 2005. **145**(1): p. 9.
- 651 84. Bennett, A.C., et al., *Larger trees suffer most during drought in forests worldwide.* *Nature*
652 *Plants*, 2015. **1**(10): p. 15139.
- 653 85. Tague, C.L., M. Moritz, and E. Hanan, *The changing water cycle: The eco-hydrologic*
654 *impacts of forest density reduction in Mediterranean (seasonally dry) regions.* *Wiley*
655 *Interdisciplinary Reviews: Water*, 2019. **6**(4): p. e1350.
- 656 86. Ma, S., et al., *Spatial variability in microclimate in a mixed-conifer forest before and after*
657 *thinning and burning treatments.* *Forest Ecology and Management*, 2010. **259**(5): p. 904-
658 915.
- 659 87. Rambo, T. and M. North, *Canopy microclimate response to pattern and density of thinning*
660 *in a Sierra Nevada forest.* *Forest ecology and management*, 2009. **257**(2): p. 435-442.

- 661 88. Nunes, A., et al., *Beneficial effect of pine thinning in mixed plantations through changes*
662 *in the understory functional composition*. Ecological engineering, 2014. **70**: p. 387-396.
- 663 89. Vesala, T., et al., *Effect of thinning on surface fluxes in a boreal forest*. Global
664 Biogeochemical Cycles, 2005. **19**(2).
- 665 90. Zausen, G., et al., *Long-term impacts of stand management on ponderosa pine physiology*
666 *and bark beetle abundance in northern Arizona: a replicated landscape study*. Forest
667 Ecology and Management, 2005. **218**(1-3): p. 291-305.

668